

Short communication

Enhanced electrochemical properties of a Si-based anode using an electrochemically active polyamide imide binder

Nam-Soon Choi*, Kyoung Han Yew, Wan-Uk Choi, Sung-Soo Kim

Energy Laboratory, Corporate R&D Center, Samsung SDI Co. Ltd., 428-5, Gongse-dong, Giheung-gu, Yongin-si, Gyeonggi-do 446-577, Republic of Korea

Received 5 November 2007; received in revised form 26 November 2007; accepted 26 November 2007
Available online 4 December 2007

Abstract

Polyamide imide (PAI), one of the classes of copolyimides containing both high mechanical properties and processibility, is used as a polymeric binder of a Si particulate electrode. The initial coulombic efficiency is improved from 28.9% (Si-PVdF) to 74.9% (Si-PAI) by introducing a PAI binder into a Si-based electrode. Variations in thickness measured at various states of charge (SOCs) and depths of discharge (DODs) indicate that the PAI binder is a much more effective restraint on volume expansion in active Si materials during the charging process than poly(vinylidene fluoride) (PVdF) binder. The discharge capacity of Si-PAI electrodes is approximately 1700 mAh g⁻¹ after 20 cycles, which is attributed to the excellent maintenance of an electrical-conducting network during cycling.

© 2007 Elsevier B.V. All rights reserved.

Keywords: Si-based electrode; Polyamide imide; PVdF; Binder; Volume expansion; FT-IR

1. Introduction

To develop rechargeable lithium batteries with high energy density, intensive studies have focused on silicon anode materials due to its extremely high lithium storage (4200 mAh g⁻¹ for Li₂₂Si₅) [1,2]. However, its cyclic performance is poor due to enormous volume changes associated with Li-ion insertion/extraction. The insertion and extraction of lithium induce mechanical strain, which causes the cracking of Si particles and loss of electrical contacts between Si and the conducting agent [3–5]. The pronounced mechanical fatigue of a Si-based anode upon prolonged cycling leads to a loss of capacity and poor cycle life. An important approach to resolving these problems is the optimization of the chemical structure of polymeric binder in a Si-based composite anode. Polymeric binder allows the electrode film to adhere to a current collector and facilitates the coherence of Si particles, which is crucial for good anode performance [6]. Apart from the requirement to maintain chemical and electrochemical stability during electrode/electrolyte interactions, polymeric binder has

to survive large repeated dimensional changes of the Si-based anode during cycling. For commercial lithium-ion batteries, poly(vinylidene fluoride) (PVdF) has generally been used as the binder for both the anode and cathode due to its good electrochemical stability [7–9]. However, the mechanical tensile strength and adhesive properties of PVdF binder are not sufficient to accommodate the significant volume changes (around 300%) in active Si material. PVdF-TFE-P binder systems, which can tolerate huge volumetric changes during charge–discharge cycling, were studied by Dahn and co-workers [10]. Additionally, an elastomeric binder was recently studied by Wu and co-workers [11] as a potential replacement for PVdF binder.

In an attempt to overcome the mechanical disintegration of a Si-based anode due to its large variation in volume during Li⁺ insertion and extraction, this study considers the introduction into Si-based anodes of polyamide imide (PAI) binder with superior mechanical and thermal properties. PAI has been commercially available for several decades and is prepared by reacting the monomer of trimellitic anhydride chloride (TMAC), obtained from the phosgenation of trimellitic acid anhydride with *m*-phenylenediamine (*m*-PDA) and 4,4'-oxydianiline (ODA) using a low-temperature solution polymerization method [12].

* Corresponding author.

E-mail address: ns75.choi@samsung.com (N.-S. Choi).

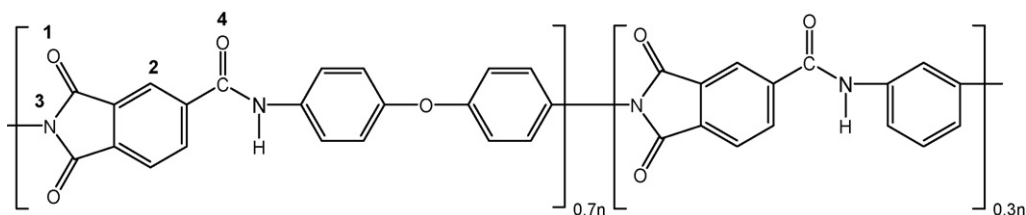


Fig. 1. Chemical structure of polyamide imide Torlon 4000 T by low-temperature solution polymerization method followed by dehydration.

This study attempts to clarify the effect of PAI binder on the electrochemical properties of Si-based anodes by using Fourier transform infrared (FT-IR) analysis and measuring the electrode thickness. Impedance spectroscopy, which helps to explain the behavior of bulk and interfacial resistance, was applied to Si composite anodes with different states of charge (SOCs) and depths of discharge (DODs). The initial coulombic efficiency was measured during the first cycle, and cycling performance was compared between Si-based anodes with PVdF or PAI binder.

2. Experimental

Polyamide imide Torlon 4000 T was obtained from Solvay Advanced Polymers; its chemical structure was characterized by Guiver and co-workers [13] and is shown in Fig. 1. To evaluate the electrochemical properties, a slurry was prepared by mixing 84 wt% silicon particles as an active material, 6 wt% super-P as an electronic conducting agent and 10 wt% binder dissolved in anhydrous *N*-methyl-2-pyrrolidinone (NMP). The resulting slurry was cast on a copper foil, and the composite electrode was dried in a convection oven at 110 °C for 2 h. The electrode was not pressed in order to obtain a proper porosity and its thickness was around 38 μm.

FT-IR spectra of the Si composite electrode obtained in various charged states and the fully discharged state were recorded from transmission measurements under a nitrogen atmosphere in a Nicolet NEXUX 870 spectrometer with a spectral resolution of 4 cm⁻¹ in the vibrational frequency range of 400–4000 cm⁻¹. After the cells reached a particular potential, they were carefully opened in a dry room, and the electrodes were rinsed in dimethyl carbonate (DMC) solvent to remove residual electrolytes and were then dried.

The tensile strength of the polymer films were measured using an Instron testing machine (Instron Co. Ltd.) and test specimens with dimensions of 9 mm × 3 mm × 0.2 mm. Volume changes during cycling are the key issue determining the electrochemical properties of Si-based electrodes. Thus, the electrode thickness was measured using a micrometer.

Coin-type half cells were used for the charge and discharge experiments, and they were assembled in an Ar-filled glove box with less than 1 ppm each of oxygen and moisture. The electrolyte solution used was 1.3 M lithium hexafluoro phosphate (LiPF₆) dissolved in a solvent mixture of ethylene carbonate (EC) and diethyl carbonate (DEC) at a 3:7 volume ratio. Charge–discharge cycling tests were galvanostatically performed at a 0.1 C rate over ranges from 70 mV to 2 V or from

5 mV to 2 V vs. Li/Li⁺ using a computer-controlled battery measurement system (TOSCAT 3000 U). To investigate the electrochemical impedance of Si composite anodes, a Solartron 1255 frequency response analyzer (FRA) was used in conjunction with a Solartron 1287 electrochemical interface over a frequency range of 10 mHz to 1 MHz.

3. Results and discussion

Fig. 2 presents the first charge–discharge curves of two Si composite anodes; one was prepared using polyamide imide and the other with the conventional poly(vinylidene fluoride) (PVdF) as a binder. The charge–discharge curve obtained with a Si electrode with PVdF binder showed a reversible capacity

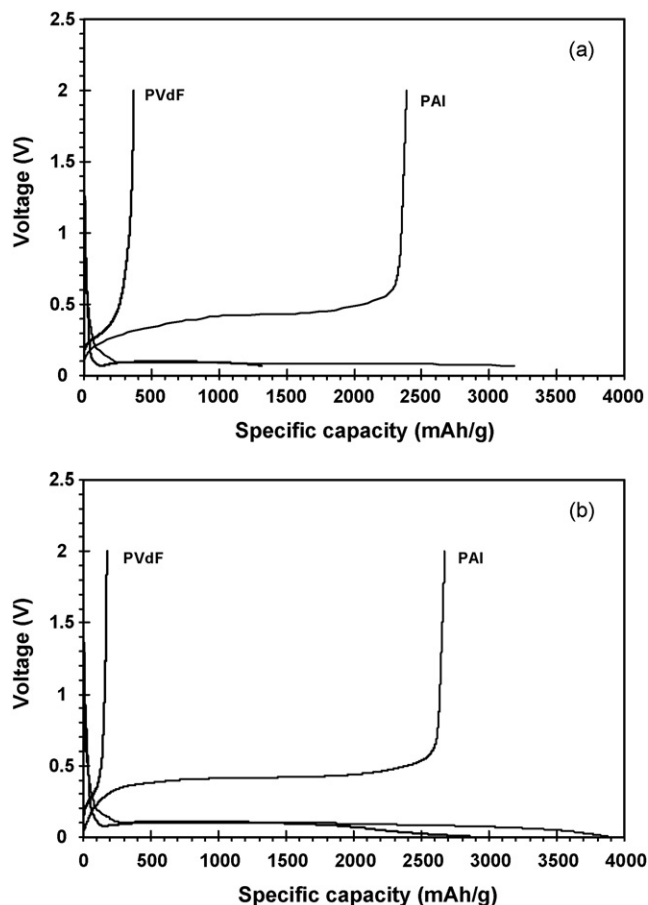


Fig. 2. Charge and discharge curves of Si-based anode in different charge potential cut-off (a) 70 mV to 2 V and (b) 5 mV to 2 V at first cycle (current density: 0.56 mA cm⁻²).

Table 1
Charge capacity and discharge capacity at pre-cycling, initial coulombic efficiency (ICE) of Si/Li coin half cell, tensile strength of polymer films, and thickness variation of Si-based anode after charge and discharge

Binder	Charge cut-off voltage (mV)	Charge capacity (mAh g ⁻¹)	Discharge capacity (mAh g ⁻¹)	ICE (%)	Tensile strength (MPa)	Thickness variation (%)	
						After charge	After discharge
PVdF	70	1313	371	28.3	18.8	221	208
	5	2856	176	6.2			
PAI	70	3189	2390	74.9	63.3	160	87
	5	3876	2674	69.0			

of approximately 371 mAh g⁻¹ at a charge cut-off potential of 70 mV. In comparison, the Si electrode with PAI binder showed a relatively high reversible capacity of 2390 mAh g⁻¹ during Li⁺ extraction. With the charge cut-off potential set at 5 mV, the reversible capacity of the Si–PAI electrode (2674 mAh g⁻¹) was greater than that of the Si–PVdF electrode (176 mAh g⁻¹), as shown in Fig. 2(b) and Table 1. Recently, our group and Christensen et al. reported that two-phase transitions appeared in two different voltage regions during Li⁺ insertion. First, the crystalline phase of Si changed to the amorphous phase between 100 mV and 70 mV. Second, amorphous changes to Li₁₅Si₄ occurred between 70 mV and 5 mV vs. Li/Li⁺ [14,15]. These phase transitions provoked a large volume expansion of the active Si material, resulting in the deterioration of the electrical-conduction network. The PAI binder plays an important role in minimizing the deterioration of the electrical contact between Si and the conducting agent. The initial coulombic efficiency of the Si–PAI electrode at charge cut-off potential of 70 mV displayed a considerable increase from 28.9% (Si–PVdF) to 74.9% (Si–PAI), as shown in Table 1.

The results of this study indicate that the intrinsic properties of a polymeric binder are closely linked to the electrochemical reversibility of Si during cycling. A comparison of the charge curves of the Si electrode indicates that the plateau appears in a Si–PAI electrode between 100 mV and 300 mV as shown in Fig. 2(a and b). This point is clearly shown in the dQ/dV graph in Fig. 3. FT-IR analysis was performed at various charged states (300 mV, 100 mV, 5 mV vs. Li/Li⁺) and a fully discharged state (2 V vs. Li/Li⁺) to quantify the reductive reaction peak of the Si electrode induced by using a PAI binder. Fig. 4 shows the FT-IR spectra of a Si–PAI electrode during Li⁺ insertion and extraction. The absorption peaks correspond to C=O stretching of an imide ring (1780 cm⁻¹ and 1720 cm⁻¹), C=O stretching of an amide group (1660 cm⁻¹ and 1580 cm⁻¹), and C–C stretching of a benzene ring (1500 cm⁻¹) of PAI in the Si–PAI electrode before cycling is observed, as depicted in Fig. 4(a). However, the absorption peaks corresponding to asymmetric and symmetric C=O stretching of an imide ring vanished at the charged state of 100 mV, as shown in Fig. 4(c). The reductive peak around 0.16 V of the Si–PAI electrode in Fig. 3 is evolved by the electrochemical reaction of the C=O group of an imide ring in a PAI binder with Li⁺ and e⁻, as shown in Fig. 4(f). Despite Li⁺ extraction from lithiated Si, the extinct C=O stretching peaks of a PAI

binder imide are not apparently shown in Fig. 4(e). Although the PAI binder reacts with Li⁺ and e⁻ during the first Li⁺ insertion, the charge and discharge capacities of the Si–PAI electrode were greatly improved, as shown in Fig. 2 and Table 1. This result indicates that the PAI binder effectively restrained the disintegration of the electronic-conduction network by the huge volume expansion of active Si materials. To further understand the need to improve the initial coulombic efficiency by using the PAI binder during the first cycle, electrochemical impedance spectroscopy (EIS) measurements were conducted at various charged and discharged states. The impedance of Si–PAI during the first Li⁺ insertion continuously decreased as depicted in Fig. 5(b), which seems to be a result of the colossal change in surface area induced by the lack of the crystalline-to-amorphous transition of Si after the first cycle [14]. During Li⁺ extraction, the impedance increased until 2 V (fully discharged state) and had a value similar to the initial impedance. However, the impedance of the Si–PVdF electrode at the 100 mV charged state vs. Li/Li⁺ increased until the 70 mV charge state vs. Li/Li⁺, as shown in Fig. 5(a). It is likely that increases in impedance by the Si–PVdF electrode can be ascribed to the deterioration of the electronic contact between the Si active material and the conducting agent due to the huge volume expansion of the Si.

The thickness of the Si–PVdF electrode drastically increased during the charge process from the initial state to 5 mV vs.

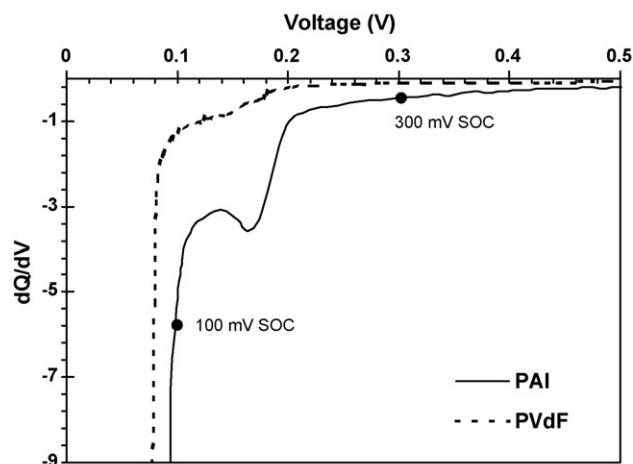


Fig. 3. dQ/dV graphs of Si-based anode at first cycle.

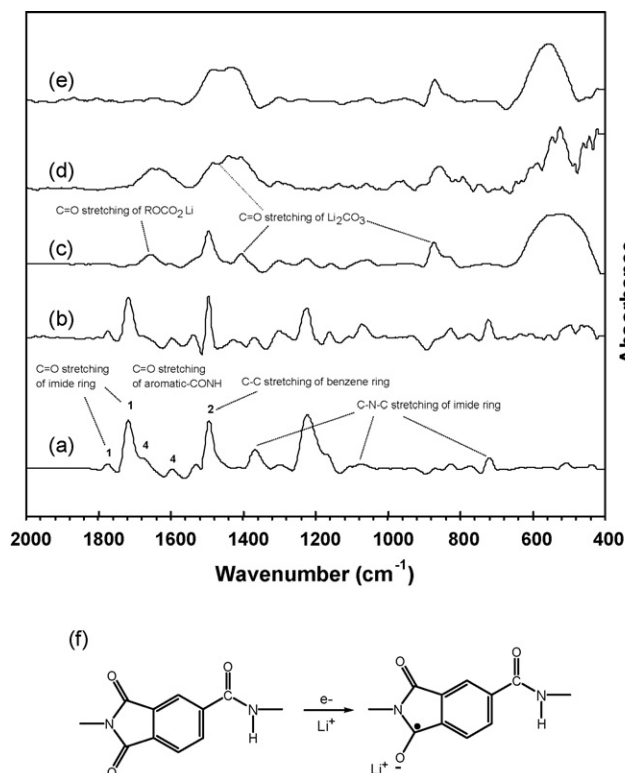


Fig. 4. FT-IR spectra of Si-based anode obtained (a) before cycling, at various charged states of (b) 300 mV, (c) 100 mV, (d) 5 mV, (e) full discharged state 2 V vs. Li/Li^+ and (f) schematic illustration for the electrochemical reaction of PAI binder with Li^+ and e^- during Li^+ insertion into Si-based anode.

Li/Li^+ , and its thickness was not recovered during the discharge process, as shown in Table 1. The trend of change in thickness was in accordance with the initial coulombic efficiency of the Si–PVdF electrode during the first charge and discharge process, as shown in Fig. 2 and Table 1. The thickness expansion ratio of a Si-based anode containing PAI binder with high tensile strength (63.3 MPa) was lower than that of the Si–PVdF electrode (18.8 MPa), and its thickness was partially recovered at the fully discharged state. From this result, we believe that the electronic-conduction network of the Si–PVdF electrode deteriorated due to the poor tensile strength of the PVdF binder, whereas that of the Si–PAI is relatively robust due to the high PAI binder tensile strength.

Electrochemical cycling tests were conducted on Si/Li coin half cells. The discharge capacity retention and coulombic efficiency of Si-based anodes with cycling is shown in Fig. 6. After the first cycle, the electrochemical reaction of Si–PVdF did not occur due to the sudden deterioration of electrical contacts between the active Si material and the conducting agent. The discharge capacity of the Si–PVdF electrode rapidly declined, and its cyclic degradation could not be eliminated by changing the charge cut-off potential from 5 mV to 70 mV. The introduction of PAI binder into Si-based anodes could lead to a considerable increase not only in the discharge capacity retention but also in the initial coulombic efficiency, as shown in Table 1 and Fig. 6, respectively. When the Si–PAI electrode was cycled in the poten-

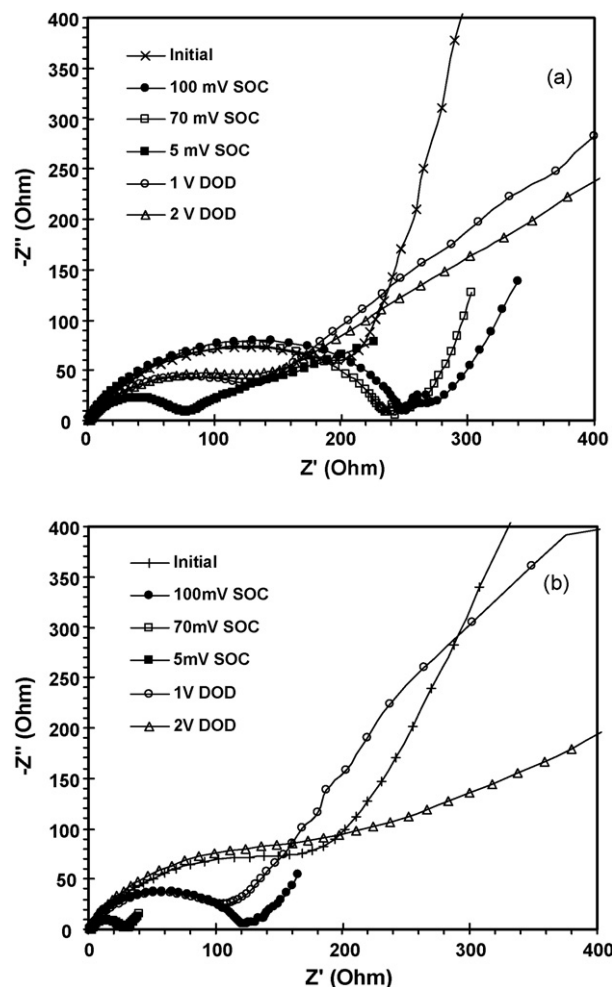


Fig. 5. Nyquist plots of Si-based anode/Li coin half cell with (a) PVdF and (b) PAI in various charged states (100 mV, 70 mV, 5 mV SOC vs. Li/Li^+) and discharged states (1 V, 2 V DOD vs. Li/Li^+).

tial region between 70 mV and 1 V vs. Li/Li^+ , which can exclude the formation of $\text{Li}_{15}\text{Si}_4$, a discharge capacity of approximately 1700 mAh g^{-1} and a coulombic efficiency of over 99.5% were obtained after 20 cycles, as shown in Fig. 6.

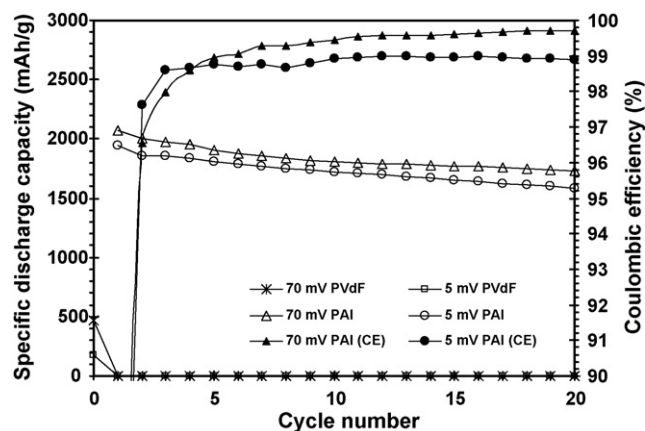


Fig. 6. Specific discharge capacity and coulombic efficiency of Si-based anode in charge–discharge potential window of 70 mV to 2 V and 5 mV to 2 V vs. Li/Li^+ .

4. Conclusions

Polyamide imide was successfully used as a binder of Si-based anode, and the electrochemical reversibility of active Si material was drastically improved by using PAI binder during cycling. The electrochemical reactivity of PAI binder in Si-based anodes was clearly elucidated by FT-IR analysis. Although PAI binder reacted with Li ions and electrons during the first charge process, the cyclic degradation of active Si material could be remarkably reduced by using PAI binder with high tensile strength. Due to the poor electrical-conducting network in Si-PVdF after Li⁺ insertion, Li ions were hardly extracted from active Si material during Li⁺ extraction, and the discharge capacity rapidly declined. These results show that a robust polymeric binder like PAI can enhance the electrochemical properties of a Si-based anode, causing large dimensional changes during cycling.

Acknowledgement

The authors would like to thank Samsung SDI Corporation for the support of this work.

References

- [1] J.P. Maranchi, A.F. Hepp, P.N. Kumta, *Electrochem. Solid State Lett.* 6 (9) (2003) A198–A201.

- [2] H. Li, X. Huang, L. Chen, Z. Wu, Y. Liang, *Electrochem. Solid State Lett.* 2 (11) (1999) 547–549.
- [3] T.D. Hatchard, J.R. Dahn, *J. Electrochem. Soc.* 151 (6) (2004) A838–A842.
- [4] Z. Chen, V. Chevrier, L. Christensen, J.R. Dahn, *Electrochem. Solid State Lett.* 7 (10) (2004) A310–A314.
- [5] M. Winter, J.O. Besenhard, *Electrochim. Acta* 45 (1999) 31–50.
- [6] H. Buqa, M. Holzapfel, F. Krumeich, C. Veit, P. Novak, *J. Power Sources* 161 (2006) 617–622.
- [7] M. Yoo, C.W. Frank, S. Mori, S. Yamaguchi, *Polymer* 44 (15) (2003) 4197–4204.
- [8] D. Guy, B. Lestriez, D. Guyomard, *Adv. Mater.* 16 (6) (2004) 553–557.
- [9] H. Huang, S.C. Yin, T. Kerr, N. Taylor, L.F. Nazar, *Adv. Mater.* 14 (2002) 1525–1528.
- [10] Z. Chen, L. Christensen, J.R. Dahn, *J. Electrochem. Soc.* 150 (8) (2003) A1073–A1078.
- [11] W.R. Liu, M.H. Yang, H.C. Wu, S.M. Chiao, N.L. Wu, *Electrochem. Solid State Lett.* 8 (2) (2005) A100–A103.
- [12] M.K. Ghosh, K.L. Mittal, *Polyimides, Fundamentals and Applications*, Marcel Dekker, New York, 1996, pp. 49–51.
- [13] G.P. Robertson, M.D. Guiver, M. Yoshikawa, S. Brownstein, *Polymer* 45 (4) (2004) 1111–1117.
- [14] Y.M. Kang, J.Y. Go, S.M. Lee, W.U. Choi, *Electrochem. Commun.* 9 (2007) 1276–1281.
- [15] M.N. Obrovac, L. Christensen, *Electrochem. Solid State Lett.* 7 (5) (2004) A93–A96.